Fluctuation and instability of steps in a diffusion field

Yukio Saito
Department of Physics, Keio University, 3-14-1 Hiyoshi, Kohoku-ku, Yokohama 223, Japan

Makio Uwaha*
Department of Physics, College of General Education, Nagoya University, Furo-cho, Chikusa-ku, Nagoya 464-01, Japan
(Received 23 July 1993; revised manuscript received 10 November 1993)

Fluctuation and morphology of steps growing in a surface diffusion field are studied theoretically and by the Monte Carlo simulation. Owing to the asymmetry in step kinetics (Schwoebel effect), a morphological instability takes place for advancing steps at a critical impingement rate f_c of gas atoms. The fluctuation of a step is reduced for receding steps with $f < f_{eq}$, and enhanced for advancing steps with $f > f_{eq}$. The width of a single step shows critical divergence at f_c. Above the instability $f > f_c$, the step motion exhibits spatiotemporal chaos, in which the crystal anisotropy influences the morphology. For a vicinal face, when the step advancement rate increases, the motion of consecutive steps is strongly correlated and the terrace width becomes stable although the fluctuation of each step is enhanced. When steps recede in sublimation, bunching of the steps is observed, which is analyzed as an instability of antiphase oscillation.

I. INTRODUCTION

Control of atomic processes is the key factor of modern crystal growth technology such as molecular- or atomic-beam epitaxy. In order to achieve good control one needs information on the structure of the crystal surface far from equilibrium as well as in equilibrium. In equilibrium the crystal surface changes its roughness with increasing temperature. For the realization of layer growth, the temperature should be kept below the roughening temperature to maintain an atomically smooth surface. In this case it is the motion of steps that determines the growth of the crystal, either on a facet or on a vicinal face. Microscopic observation of the crystal surface and steps at an atomic scale has become possible[1–4] with the invention of the scanning tunneling and atomic force microscopes (STM, AFM) as well as the recent development of various electron microscopes. There are comprehensive studies on the equilibrium fluctuation of steps and microscopic understanding of step tension and a step-step interaction is obtained.[5–8]

Out of equilibrium the step morphology is influenced not only by the static properties but also by dynamical processes. In crystal growth from a vapor, the exchange of atoms between the crystal and the ambient vapor controls the spatial uniformity of the system. On the other hand, surface diffusion of adsorbed atoms on an atomically smooth surface is essential in determining the step shapes, and the quality of the crystal as a result. The linear stability analysis by Bales and Zangwill[9] shows that straight steps become unstable in a surface diffusion field when they advance faster than a critical velocity. The step fluctuation is also influenced by the kinetics: it increases drastically on approaching the critical velocity, while it decreases as the step recedes.[10] We studied a step model on a lattice with a solid-on-solid (SOS) restriction by means of a Monte Carlo simulation.[10–13] The SOS condition states that the step position $y(x)$ is a single-valued function of the coordinate along the average step orientation x [as a result, the height of the surface $z(x,y)$ is also a single-valued function of (x,y)]. Hence the step neither folds back to form an overhang nor tears off. This condition is valid for a step with a small deviation from the straight line, but near the instability point it becomes inadequate for representing a real system. In the present paper we perform simulations without the SOS restriction and confirm the previous results for the fluctuation of a moving step.[10] Without the restriction, we can study the morphology of an unstable step as well. We find that steady growth is not possible in this system. The structure we get shows spatiotemporal chaotic behavior, and is very different from the array structure of cells or dendrites observed in unidirectional solidification.[14,15]

For a vicinal surface with equidistant steps, step interaction via the diffusion field carries novel features in the global morphology of the step system. When steps are advancing, in-phase fluctuations of neighboring steps are enhanced compared to the equilibrium state and morphological instability takes place similarly to that of a single step. On the contrary, we show that during growth the fluctuation of step separation is suppressed by the interference of the diffusion field. When the steps are receding, on the other hand, antiphase fluctuation of neighboring steps are enhanced to produce a bunching instability of neighbor step pairs.[16–18]

II. STABILITY OF A STRAIGHT STEP

We consider crystal growth from a vapor. A gas atom impinges on the surface of a growing crystal, diffuses on

the surface, and evaporates back into the ambience after a certain lifetime. Assuming that the temperature of the crystal is lower than the roughening temperature of the surface concerned, crystal growth takes place at steps on the surface, and steps act as sources or sinks for the diffusion field of the adsorbed atoms (which will be abbreviated adatoms hereafter). As in the standard Burton-Cabrera-Frank model,[19] concentration of the adatoms, $c(\mathbf{r},t)$, on the crystal surface varies according to the diffusion equation, with impingement from an ambient vapor and evaporation from the substrate, as

$$\frac{\partial c}{\partial t} = D_s \nabla^2 c + f - \frac{c}{\tau}. \tag{1}$$

Here D_s is the surface diffusivity, f is the impingement rate of atoms on a unit surface area per unit time, and τ is the lifetime of an adatom until evaporation.

We consider a descending step on a crystal surface. Far from the step, the impingement and the evaporation are balanced and the concentration is expected to become constant as $c_\infty = \tau f$. At the step, the adatoms solidify and the mass deficiency produced should be supplied by the diffusion flux as

$$\Omega^{-1} v_n = D_s(\partial_n c|_+ - \partial_n c|_-), \tag{2}$$

where Ω is the atomic area, v_n is the normal step velocity at the interface, and $\partial_n c|_+$ ($\partial_n c|_-$) is the normal derivative of the concentration in front (in the rear) of the step. Another boundary condition is a linear response of the growth rate to step supersaturation. By taking into account the asymmetry in step kinetics (the Schwoebel effect[20]), the growth rate is expressed as,[9]

$$\Omega^{-1} v_n = K_+(c_{i+} - c_{\rm eq}) + K_-(c_{i-} - c_{\rm eq}). \tag{3}$$

K_+ (K_-) is the kinetic coefficient for growth from the front (rear) terrace, c_{i+} (c_{i-}) the interfacial adatom concentration in front (in the rear) of the step, and $c_{\rm eq}$ is the equilibrium adatom concentration for a curved step, with Gibbs-Thomson effect included as

$$c_{\rm eq} = c^0_{\rm eq} + \frac{\Omega c^0_{\rm eq} \tilde{\beta}}{k_B T}\kappa. \tag{4}$$

$c^0_{\rm eq}$ is the equilibrium concentration for a straight step, $\tilde{\beta}(= \beta + \beta'')$ the step stiffness, k_B the Boltzmann constant, T the temperature, and κ the curvature of the step.

When the step grows, keeping its shape straight, the concentration field depends on the y coordinate, perpendicular to the step. The growth of a step is normally slow enough for the diffusion field to relax to the stationary distribution, given as a solution for $\partial c/\partial t = 0$ with the instantaneous boundary conditions. In this stationary approximation, the concentration field is obtained as

$$c_\pm(y) = c_\infty - \frac{c_\infty - c^0_{\rm eq}}{D_s/x_s K_\pm + 1} e^{\mp y/x_s}. \tag{5}$$

c_+ (c_-) represents the field in front, $y > 0$, (in the rear, $y < 0$) of the step, and $x_s \equiv \sqrt{D_s \tau}$ is the surface diffusion length. The growth velocity is proportional to the supersaturation $c_\infty - c^0_{\rm eq}$, as

$$v_0 = \Omega K_{\rm eff}(c_\infty - c^0_{\rm eq}), \tag{6}$$

with the effective kinetic coefficient

$$K_{\rm eff} = (K_+^{-1} + x_s/D_s)^{-1} + (K_-^{-1} + x_s/D_s)^{-1}. \tag{7}$$

The step stops growing when the impingement rate f takes the equilibrium value $f_{\rm eq} = c^0_{\rm eq}/\tau$.

The growth rate v can also be expressed as a function of the chemical potential difference $\Delta\zeta$ between the adatom and the solid atom. Assuming the adatoms to be an ideal gas, its chemical potential is written as $\zeta_{\rm ad} = k_B T \ln c_\infty$. The chemical potential of the solid is the same as that of the equilibrium adatom, $\zeta_{\rm sol} = k_B T \ln c^0_{\rm eq}$. Thus the chemical potential difference is obtained as $\Delta\zeta = k_B T \ln(c_\infty/c^0_{\rm eq}) \approx k_B T(c_\infty/c^0_{\rm eq} - 1)$. For a small $\Delta\zeta$, the step velocity is proportional to the driving force $\Delta\zeta/\Omega$ with the proportionality coefficient μ_0, the mobility. In the present case of Eq. (6), the step mobility is obtained as

$$\mu_0 = \Omega^2 \frac{K_{\rm eff} c^0_{\rm eq}}{k_B T}. \tag{8}$$

We now consider the stability of a straight step in steady motion. For simplicity we assume that the step grows only from the lower terrace, and that local equilibrium in front of the step is realized: $K_- = 0$ and $K_+ = \infty$. We again use the stationary approximation, in which the diffusion field is assumed to follow the step motion instantaneously. (We will discuss the effect of finite kinetic coefficients $K_\pm$ and corrections to the stationary approximation in the next section.) By linear analysis with a small sinusoidal perturbation of the step position,

$$y(x,t) = v_0 t + \delta y_k e^{\omega_k t} \cos kx, \tag{9}$$

the amplification rate of the perturbation is obtained as

$$\omega_k = -k^2 \tilde{\beta} \Omega^2 \frac{c^0_{\rm eq}}{k_B T} D_s \Lambda_k + v_0(\Lambda_k - \Lambda_0), \tag{10}$$

where

$$\Lambda_k = \sqrt{k^2 + x_s^{-2}}. \tag{11}$$

This formula can be interpreted as the amplification rate being a product of an effective k-dependent step mobility

$$\mu_k = \Omega^2 \frac{c^0_{\rm eq}}{k_B T} D_s \Lambda_k, \tag{12}$$

and an effective force constant

$$\nu_k(f) = \tilde{\beta}\left[k^2 - \frac{1}{\xi x_s}\left(1 - \frac{1}{x_s \Lambda_k}\right)\right], \tag{13}$$

where ξ is the radius of a two-dimensional critical nucleus,

$$\xi \equiv \frac{\Omega\tilde{\beta}}{\Delta\zeta} = \frac{\Omega c_{\rm eq}^0 \tilde{\beta}}{k_B T(c_\infty - c_{\rm eq}^0)} = \frac{\Omega f_{\rm eq}\tilde{\beta}}{k_B T(f - f_{\rm eq})}. \quad (14)$$

This quantity becomes negative if $f < f_{\rm eq}$, that is, in sublimation of the crystal. The mobility μ_k is independent of the impingement rate f, and in the long-wavelength limit $\mu_{k=0}$ is the mobility μ_0 appearing in the growth rate v_0.

For small k, $\omega_k(f)$ can be expanded as

$$\omega_k(f) = -\mu_0\left[\tilde{\beta}\left(1 - \frac{x_s}{2\xi}\right)k^2 + \tilde{\beta}\left(\frac{1}{2} + \frac{x_s}{8\xi}\right)x_s^2 k^4\right], \quad (15)$$

and the coefficient of the first term

$$\tilde{\beta}_{\rm eff} = \tilde{\beta}\left(1 - \frac{x_s}{2\xi}\right) = \tilde{\beta}\frac{f_c - f}{f_c - f_{\rm eq}} \quad (16)$$

may be called the effective step stiffness. For small f where $\tilde{\beta}_{\rm eff} > 0$, the amplification rate of the perturbation ω_k is negative for all values of the wave number k, and the perturbation dies out eventually. But when the the radius of the critical nucleus ξ is smaller than $x_s/2$ or the impingement rate f is larger than the critical value

$$f_c = f_{\rm eq}\left(1 + \frac{2\tilde{\beta}\Omega}{k_B T x_s}\right), \quad (17)$$

the effective stiffness $\tilde{\beta}_{\rm eff}$ is negative and the amplification rate ω_k becomes positive for small values of k between zero and $k_c \approx \sqrt{4/3(x_s/2\xi - 1)}x_s^{-1}$. Thus the step cannot keep its straight shape for $f > f_c$ due to the pointing effect of the diffusion field. The growth rate of the perturbation ω_k is maximum at

$$k_{\rm max} = \sqrt{\frac{2}{3}\left(\frac{x_s}{2\xi} - 1\right)}\frac{1}{x_s}, \quad (18)$$

which is approximately $k_c/\sqrt{2}$, and the mode with $k = k_{\rm max}$ is the most unstable mode. Note that well above the critical point the wavelength of the most unstable mode is proportional to the geometrical average of the surface diffusion length and the radius of the critical nucleus: $\lambda_{\rm max} = 2\pi\sqrt{3\xi x_s}$. The morphology of a step in this case is studied later, in Sec. VI.

III. ASYMMETRY IN STEP KINETICS

We first examine the validity and limitation of the simplification and the approximation we have made in the previous section. In order to emphasize the Schwoebel effect we adopted the simplification of the extremity of the asymmetric model, that is $K_- = 0$ and $K_+ = \infty$, and obtained the simple formulas (12) and (13). With arbitrary values of K_- and K_+, the growth rate ω_k of a sinusoidal perturbation becomes[9]

$$\omega_k(f; d_+, d_-) = -\mu_k(d_+, d_-)\nu_k(f; d_+, d_-), \quad (19)$$

where

$$d_\pm \equiv D_s/K_\pm \quad (20)$$

characterizes the relevance of the step kinetics in the growth. Here the k-dependent mobility is generalized as

$$\mu_k(d_+, d_-) = \Omega^2\frac{c_{\rm eq}^0}{k_B T}D_s\Lambda_k\left(\frac{1}{1 + d_-\Lambda_k} + \frac{1}{1 + d_+\Lambda_k}\right), \quad (21)$$

and the effective force constant as

$$\nu_k(f, d_+, d_-) = \tilde{\beta}\left[k^2 - \frac{1}{\xi(f; d_+, d_-)x_s}\left(1 - \frac{1}{x_s\Lambda_k}\right) \times\left(1 + \frac{x_s\Lambda_k - 1}{2 + (d_+ + d_-)\Lambda_k}\right)\right], \quad (22)$$

with the generalized ξ

$$\xi(f; d_+, d_-) = \frac{\Omega c_{\rm eq}^0\tilde{\beta}}{k_B T\Delta c_i(f; d_+, d_-)}, \quad (23)$$

which depends on the density gap across the step,

$$\Delta c_i \equiv c_{i-} - c_{i+} = \left(\frac{1}{1 + d_+/x_s} - \frac{1}{1 + d_-/x_s}\right)(c_\infty - c_{\rm eq}^0), \quad (24)$$

and no longer has the meaning of the radius of the two-dimensional critical nucleus. For small k, ω_k can be written as

$$\omega_k = -\mu_0\tilde{\beta}\left(1 - \frac{x_s}{2\xi(f, d_+, d_-)}\right)k^2, \quad (25)$$

with μ_0 defined by Eq. (8). Thus the qualitative features do not change as long as the asymmetry in step kinetics exists with nonzero Δc_i. It is the density gap across the step Δc_i that determines the nonequilibrium effect of surface diffusion.

For symmetric step kinetics, $K_- = K_+$, stability seems to be recovered in the stationary approximation, because $\Delta c_i = 0$, $\xi = \infty$, and ω_k remains always negative. But with a better approximate treatment of the diffusion equation, we find that the instability can still take place. There is an asymmetry in the forward and backward directions of the step since it is in motion. In the steady-state approximation of the diffusion field, we assume that the density profile is stationary in the frame of a *moving* step. In the case of fast kinetics $K_- = K_+ = \infty$, the characteristic lengths of the density variation in front and in the rear of the step are the reciprocal of the wave number

$$\kappa_\pm = \sqrt{x_s^{-2} + l_D^{-2}} \pm l_D^{-1}. \quad (26)$$

Here $l_D = 2D_s/v_0$ is the ordinary diffusion length, and v_0 is the growth velocity of a straight step, given now by

$$v_0 = 2\frac{D_s}{x_s}\frac{c_\infty - c_{\rm eq}^0}{\sqrt{\Omega^{-2} - (c_\infty - c_{\rm eq}^0)^2}}. \tag{27}$$

The density gradient is always larger in the direction of movement of the step. When the step velocity is fast enough, this asymmetry becomes another source of instability. The growth rate of a step perturbation is calculated as $\omega_k = -\tilde{\mu}_k\tilde{\nu}_k$ with

$$\tilde{\mu}_k = 2\Omega^2\frac{c_{\rm eq}^0}{k_BT}D_s\tilde{\Lambda}_k \tag{28}$$

and

$$\tilde{\nu}_k = \tilde{\beta}\left[k^2 - \frac{1}{\xi l_D}\left(1 - \frac{\tilde{\Lambda}_0}{\tilde{\Lambda}_k}\right)\right], \tag{29}$$

with ξ defined by Eq. (14) to be finite even for $K_+ = K_- = \infty$, and

$$\tilde{\Lambda}_k \equiv \sqrt{k^2 + x_s^{-2} + l_D^{-2}}. \tag{30}$$

For small k, $\tilde{\nu}_k$ can be expanded as

$$\tilde{\nu}_k = \tilde{\beta}\left(1 - \frac{1}{2\tilde{\Lambda}_0^2 l_D\xi}\right)k^2. \tag{31}$$

Since $(\xi l_D)^{-1} \propto (f - f_{\rm eq})^2$, the instability takes place for both advancing and receding steps in this better approximation. However, if there is an asymmetry in kinetic coefficients, for instance $K_+ > K_-$, then the stabilization due to the Schwoebel effect on the receding step is stronger than the above instability, and the straight step can recede stably.

IV. FLUCTUATION OF A STEP

We now continue our investigation with the most asymmetric one-sided model, $K_- = 0$ and $K_+ = \infty$. Even in the region $f < f_c$ where a straight step is stable, the instantaneous shape of a step is not strictly straight but fluctuates because of the thermal noise. We here summarize our previous investigation[10] on the effect of diffusion kinetics on the step fluctuation.

A sinusoidal perturbation of the interface is written as $y(x,t) = v_0t + \delta y_k(t)\cos kx$. The effect of thermal noise may be described by a random force $R_k(t)$ with zero mean $\langle R_k(t)\rangle = 0$ in the Langevin equation for δy_k,

$$\delta\dot{y}_k(t) = \mu_k[-\nu_k(f)\delta y_k(t) + R_k(t)]. \tag{32}$$

The random force is assumed to have the spectrum $\langle R_k(t)R_{k'}(t')\rangle = G_k\delta_{k+k'}\delta(t-t')$. The linear equation (32) can be solved easily[21] and the correlation function can be calculated for an initially straight step[10]

$$\langle\delta y_k(t)\delta y_{k'}(t)\rangle = \frac{\mu_kG_k}{2\nu_k(f)}\delta_{k+k'}(1 - e^{-2\mu_k\nu_kt}). \tag{33}$$

By imposing the condition[22] that at $f = f_{\rm eq}$ the steady-state correlation function should take the equilibrium value which satisfies the equipartition law as $\langle\delta y_k\delta y_{k'}\rangle = (T/\tilde{\beta}k^2)\delta_{k+k'}$, we obtain the noise spectrum G_k as $G_k = 2k_BT/\mu_k$. With the same noise spectrum, the nonequilibrium correlation function in the steady state becomes

$$\langle|\delta y_k|^2\rangle = k_BT/\nu_k(f). \tag{34}$$

For $f < f_c$ where $\tilde{\beta}_{\rm eff}$ is positive, the step width w defined by $w^2 \equiv \langle[\delta y(x)]^2\rangle$ behaves as

$$w^2 = \frac{1}{L}\sum_k\langle|\delta y_k|^2\rangle = \frac{LT}{12\tilde{\beta}_{\rm eff}} = \frac{LT}{12\tilde{\beta}}\frac{f_c - f_{\rm eq}}{f_c - f}. \tag{35}$$

Here L is the size of the system in the x direction where a periodic boundary condition is imposed. The effective stiffness (16) increases as the impingement frequency f is decreased, and, as a result, a receding step is smoother than an equilibrium one. On the contrary, as f is increased, $\tilde{\beta}_{\rm eff}$ decreases, and an advancing step fluctuates more than an equilibrium step. Since the effective stiffness $\tilde{\beta}_{\rm eff}$ vanishes on approaching f_c, the width diverges near f_c as $w^2/L \propto (f_c - f)^{-1}$. This critical divergence of the fluctuation is similar to that in a static phase transition. We study this suppression and enhancement of the fluctuation by Monte Carlo simulation of a lattice-gas model in the next section.

V. MONTE CARLO SIMULATION

Our simulation system is a square lattice of size $L \times H$ with the lattice constant $a = 1$. An integer height variable $z(x,y)$ is asigned on each lattice site, representing the height of the crystal. Initially, the system contains n steps running parallel to the x axis, and the height decreases on traversing the step in the y direction. We call this a [10] step hereafter. The boundary condition in the y direction is thus $z(x, y+H) = z(x,y) - n$, and in the x direction a periodic boundary condition $z(x+L, y) = z(x,y)$ is imposed. The average separation of the neighboring steps is $l = H/n$.

Gas atoms impinge on top of the crystal with a frequency f and are adsorbed on it. When an adatom among N_a of them performs a random walk on the crystal surface, the time increases $(4N_a)^{-1}$ for each diffusion trial. In these units the diffusion constant D_s takes the value 1. An adatom desorbs into the ambient with a lifetime τ. During diffusion, when an adatom touches a step from the lower terrace, it tries to solidify with a probability $p_s = [1 + \exp(\Delta E_s - \phi)/k_BT]^{-1}$. Here E_s is the step energy, $E_s = \epsilon\times$ step perimeter, ϕ is the chemical potential gain by solidification, and T is the temperature of the crystal. To satisfy the detailed balance, the solid atoms at step sites remelt to become an adatom with a probability $p_m = [1 + \exp(\Delta E_s + \phi)/k_BT]^{-1}$. From these data one can calculate physical quantities such as

the step stiffness $\tilde{\beta}_{[10]}$ as[23]

$$\frac{k_BT}{\tilde{\beta}_{[10]}} = \frac{2e^{-\epsilon/k_BT}}{(1-e^{-\epsilon/k_BT})^2}, \tag{36}$$

and the equilibrium adatom density

$$c_{\rm eq}^0 = \frac{1}{1+e^{\phi/k_BT}}. \tag{37}$$

Figure 1 shows the time evolution of a single step at various impingement rates f. The solid-on-solid conditon is not imposed so that step overhangs are allowed. The system size is chosen to be $L \times H = 256 \times 128$, but the views in Fig. 1 are extended in the y direction. The kink energy ϵ is taken as ϵ/k_BT=2.0, the chemical potential gain $\phi/k_BT = 2.0$, and the lifetime of the adatom is $\tau = 256$. The step stiffness is then calculated as $k_BT/\tilde{\beta}_{[10]} = 0.362$, the equilibrium density $c_{\rm eq}$=0.119, the equilibrium impinging rate $f_{\rm eq} = 4.65\times10^{-4}$, the critical impinging rate $f_{c,[10]} = 6.26\times10^{-4}$, and the diffusion length $x_s = \sqrt{D_s\tau} = 16$, much shorter than the system size $L = 256$ or H=128. The frequency of solidification-melting trial in our simulation algorithm corresponds to $K_+ = 4$. This value is much larger than $D/x_s = 1/16$ and the simulation is considered as the case of fast step kinetics. With f smaller than the equilibrium value, the crystal is sublimating and the step is receding, as is shown in Fig. 1(a). At the equilibrium impingement rate $f_{\rm eq}$ the step stops growing. For f larger than $f_{\rm eq}$ the step grows forward. Until $f_{c,[10]}$ the straight step remains stable [Fig. 1(b)], whereas for $f > f_{c,[10]}$ the step develops deep grooves [Fig. 1(c)]. The analysis of the step morphology for $f > f_{c,[10]}$ will be described later.

Here we summarize the growth and morphology of the stable straight step below $f_{c,[10]}$. The step velocity is shown in Fig. 2(a), where our previous simulation result of a SOS step without overhangs is also plotted. The velocity vanishes at the equilibrium $f_{\rm eq}$, and follows very well the theoretical curve without any adjustable parameter up to $f_{c,[10]}$. For $f > f_{c,[10]}$ the deviation from the theoretical curve is evident, indicating the speeding up caused by step fluctuation. Figure 2(b) shows the normalized width as a function of the impingement rate f. Monte Carlo data points clearly indicate the suppression of the step fluctuation in sublimation, and its enhancement in growth. Theoretically, divergence of the width $w/\sqrt{L}$ is expected at $f_{c,[10]}$ for $L \to \infty$ as indicated by the curves, but the width simulated for a finite system remains finite. One only observes that $w/\sqrt{L}$ near $f_{c,[10]}$ increases on increasing the system width L. The finiteness of the system size introduces the minimum wave number, $k_{\rm min} = 2\pi/L$. At $k_{\rm min}$ the quartic term in Eq. (15) becomes comparable to the quadratic term when f approaches $f_{c,[10]}$. Then a deviation of $w/\sqrt{L}$ from the value of an infinite system is expected. Comparing the two terms of Eq. (15) at $k_{\rm min}$, we can estimate when the deviation occurs. For our small system with $L = 64$, which is only four times larger than $x_s = 16$, the deviation occurs already around $f \approx f_{\rm eq}$, in agreement with the plot in Fig. 2(b). For a larger system with $L = 256$, the deviation is expected around $f \approx 6.1 \times 10^{-4}$, also

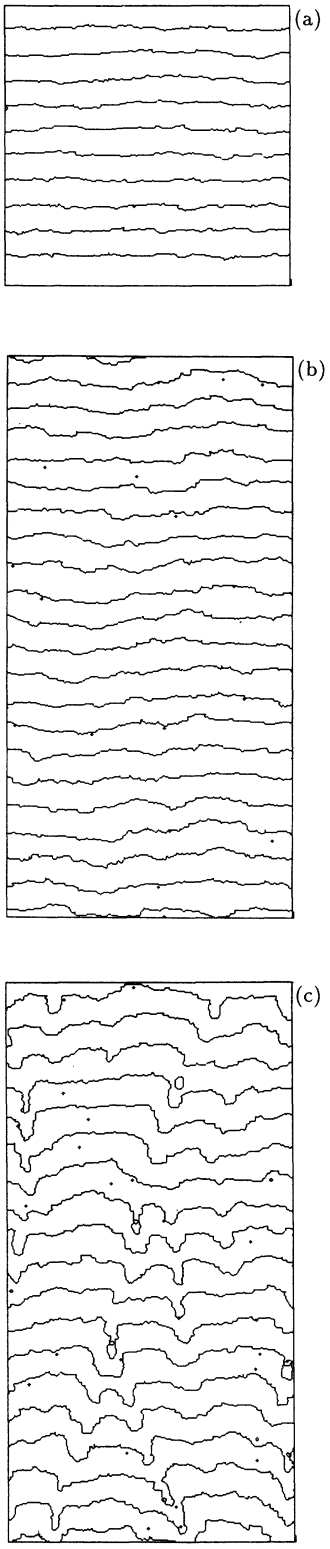

FIG. 1. Time evolution of a single [10] step on a square lattice with parameters $\epsilon/k_BT = \phi/k_BT = 2$, $D_s = 1$, and $\tau = 256$ ($x_s = 16$). Impingement rate is (a) $f = 3 \times 10^{-4}$, (b) $f = 6 \times 10^{-4}$, and (c) $f = 8 \times 10^{-4}$. The step in (a) is receding downward, whereas steps in (b) and (c) are advancing upward. The width shown is 256, and the heights are 256 for (a) and 512 for (b) and (c). The simulated system size is $L \times H = 256 \times 128$.

in agreement with Fig. 2(b). For a systematic study of the finite-size effect on the critical divergence of the step width $w/\sqrt{L}$, simulations for various system sizes are necessary. Since we are dealing with diffusion dynamics, however, simulation for a large system requires very long computation, which yet remains to be done.

In real space the correlation function (34) gives the difference of the step position as

$$h(x) \equiv \langle [\delta y(x+x',t) - \delta y(x',t)]^2 \rangle = \frac{2k_BT}{L} \sum_k \frac{1-\cos kx}{\nu_k(f)}, \tag{38}$$

which becomes the usual parabolic form $(k_BT/\tilde{\beta})x(L-x)/L$ at equilibrium. If f is different from f_{eq}, the curve is no longer a parabola. For short distances $h(x)$ is determined by ν_k at large wave numbers and is insensitive to the impingement rate f. On the other hand, the large-distance behavior is determined by ν_k at small k, and

$$h(x) \approx \frac{k_BT}{\tilde{\beta}_{\text{eff}}} x \tag{39}$$

for the infinite system. Figure 3 shows the simulation results of SOS step for $f = 3\times10^{-4}$, $f = f_{eq} = 4.65\times10^{-4}$, and $f = 6\times10^{-4}$, in comparison with the theoretical curves calculated by Eq. (38). The predicted features are observed in the simulation although the agreement is qualitative. Theoretical values with k summation for the small system size underestimate the fluctuation effect. This is also the case for the width $w/\sqrt{L}$, if one limits the k summation in (35) to finite wave numbers.

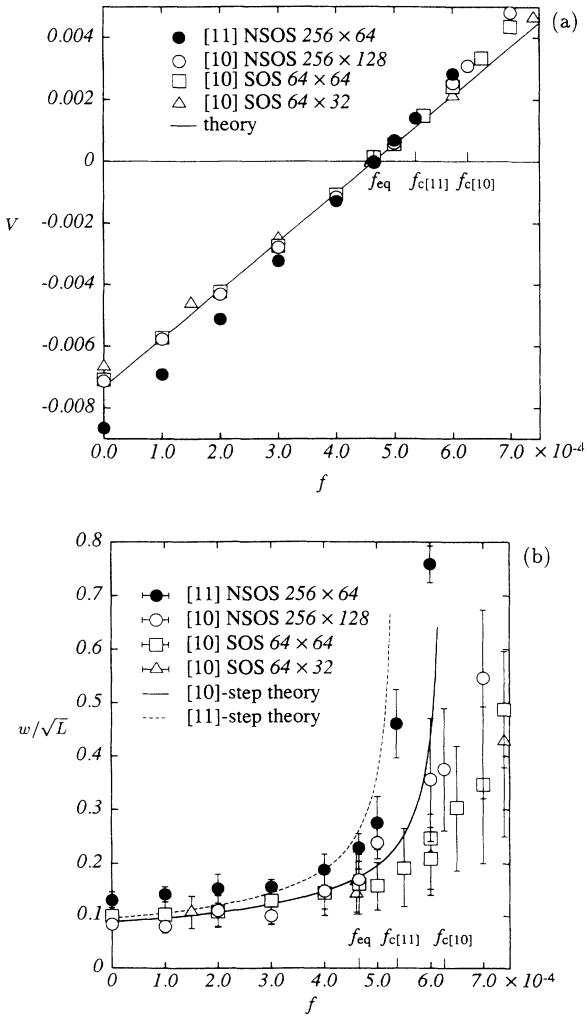

FIG. 2. (a) Velocity and (b) width of a single step aligned in the [10] and [11] orientations versus the impingement rate f. Simulation results of non-solid-on-solid (NSOS) steps as well as the previous solid-on-solid (SOS) steps in various orientations in systems of various sizes $L \times H$ are shown and compared with the theoretical result.

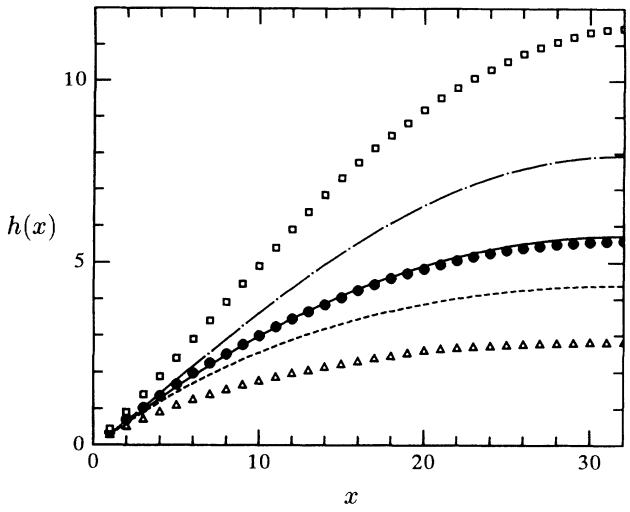

FIG. 3. Correlation along the step, $h(x) \equiv \langle [\delta y(x+x') - \delta y(x')]^2 \rangle$, versus the separation x. The impingement rates are $f = 3\times10^{-4}$, $f = f_{eq} = 4.65\times10^{-4}$, and $f = 6\times10^{-4}$, from bottom to top. The data points are simulation results for the SOS step in a system of size 64×64, and the lines are the theoretical calculation.

VI. MORPHOLOGY OF AN UNSTABLE STEP

A. Spatiotemporal chaos

When the impingement rate f exceeds the critical value $f_{c,[10]}$, a straight step is unstable for sinusoidal perturbations with wave vectors k between 0 and k_c. What kind of morphology then would the step take when it becomes unstable? Would the step take a periodic structure with, for example, the most unstable wave vector k_{max}? The time evolution of the step profile is shown in Fig. 1(c) for $f = 8\times10^{-4}$. The morphology is characterized by many grooves between the almost flat fronts. The separation of grooves is of the order of the periodicity of the most unstable mode, $\lambda_{max} = 2\pi/k_{max}$, which is 118 for $f = 8\times10^{-4}$. The structure is, however, not at all stationary but is very irregular in space and time. Grooves meander transversely to the left or to the right, and collide irregularly with the neighboring grooves, to be an-

nihilated. When the separation between two grooves increases, the flat front becomes unstable and a new groove is created. For larger f, such as $f = 10 \times 10^{-4}$ (not shown), we also observed similar nonstationary grooves with separations of order $\lambda_{\max} = 81$. This kind of creation, collision, and annihilation of grooves, irregular in space and time, is also observed in experiments on directional viscous fingering,[24] and the phenomenon is called spatiotemporal chaos.

The problem then is to understand whether this chaotic behavior is an intrinsic behavior of the system or is an effect caused by noise. Bena, Misbah, and Valance have studied the nonlinear evolution of a step near the critical point with perturbation theory and predicted a chaotic behavior.[25] Near the critical point f_c we have a small parameter $\epsilon \equiv -\tilde{\beta}_{\rm eff}/\tilde{\beta}$. The wave vector $k_{\max}$ which characterizes the spatial structure is proportional to the square root of ϵ, and the time is characterized by the largest amplification rate $\omega_{k_{\max}}$ which is proportional to the square of ϵ. Therefore, by introducing the new space coordinate $\tilde{x} = \epsilon^{1/2}x/x_s$ and the new time coordinate $\tilde{t} = \epsilon^2 t\mu_0\tilde{\beta}/x_s^2$, and expanding the step deformation and the diffusion field as $Y(\tilde{x},\tilde{t}) \equiv (y(x,t) - v_0 t)/x_s = \epsilon Y_1 + \epsilon^2 Y_2 + \epsilon^3 Y_3 + \cdots$, and $c = c_0 + \epsilon c_1 + \epsilon^2 c_2 + \epsilon^3 c_3 + \cdots$, respectively, one obtains the following evolution equation for Y_1 from the solvability condition up to order ϵ^3:

$$\frac{\partial Y_1}{\partial \tilde{t}} = -2\frac{\partial^2 Y_1}{\partial \tilde{x}^2} - \frac{3}{4}\frac{\partial^4 Y_1}{\partial \tilde{x}^4} + \left(\frac{\partial Y_1}{\partial \tilde{x}}\right)^2. \tag{40}$$

This is a form of the Kuramoto-Sivashinsky (KS) equation.[26,27]

The KS equation has been studied in the field of nonlinear dynamics, and is known as an example of a deterministic system which shows spatiotemporal chaotic behavior.[28,25] Numerical solution of the KS equation shows creation, collision, and annihilation of bumps, similar to our lattice-gas Monte Carlo simulation. Therefore, the spatiotemporal chaotic behavior found in our system is most likely to be an intrinsic phenomenon and not an effect induced by noise. For the KS equation it is known that the system size should be rather large to gain spatiotemporal chaos, whereas our system shows the chaotic behavior even with a small system size. This may be due to the noise inherent in our system.

B. Effect of crystal anisotropy

In dendritic crystal growth, it is believed that anisotropy is important to maintain the regular profile of the interface. Without the anisotropy, the solidification front in the diffusion field is unstable to the perpetual tip splitting and this results in an irregular form. With anisotropy of the surface tension, the tip oriented in the direction of the minimum step stiffness is believed to be stable.[29]

In the previous section, we found that the step running in the [10] direction shows spatiotemporal chaos with random occurrence of tip splitting. This is a direction of maximal stiffness, and the tip stabilization effect due to anisotropy is not expected. Following the analogy to dendritic growth, the anisotropy stabilizes the step advancing in the direction of minimal step stiffness, namely, in the diagonal [11] direction of the square lattice. A statistical mechanics calculation of the step stiffness yields[30]

$$\frac{k_B T}{\tilde{\beta}_{[11]}} = \frac{1}{\sqrt{2}}\frac{(1+e^{-2\epsilon/k_BT})^2 + 4e^{-2\epsilon/k_BT}}{(1-e^{-2\epsilon/k_BT})^2}, \tag{41}$$

which gives an inverse stiffness $k_BT/\tilde{\beta}_{[11]} = 0.815$, larger than the corresponding stiffness in the [10] direction, $k_BT/\tilde{\beta}_{[10]} = 0.362$. The perturbative calculation in the previous section is insensitive to anisotropy up to the order of ϵ^3, but the validity of the perturbation theory is limited near f_c and the anisotropy may change the chaotic behavior in higher order of ϵ.

Monte Carlo simulation of a step advancing in the diagonal direction is performed for a system with a square lattice rotated by 45° into the [11] direction. The system size $L \times H$ for the [11]-step simulation means that the side length in the x direction is $L/\sqrt{2}$ and that in the y direction is $\sqrt{2}H$. First we investigate the orientation dependence in the step velocity and width, and the results are shown in Fig. 2. A step does not grow at the equilibrium impingement rate $f_{\rm eq}$, indicating the validity of our simulation to reproduce the equilibrium state. In Fig. 2(a) the receding velocity of a [11] step is larger than that of a [10] step. This is because the [11] step is rougher than the [10] step, as is evident by comparing Figs. 1(a) and 4(a). For an advancing step, the [11] step becomes unstable more easily than the [10] step, since the stability limit f_c depends on the step stiffness: $f_{c,[11]} = 5.36 \times 10^{-4}$ whereas $f_{c,[10]} = 6.26 \times 10^{-4}$. This is evident from the width enhancement in the [11] direction for large f in Fig. 2(b).

After the instability has taken place, a [11] step moves steadily with a pointed tip, as is shown in Fig. 4(c). The [11] tip at $f = 8 \times 10^{-4}$ looks more stable than the [10] step at the same f, but the groove is not deep and wide enough to produce sidebranches, since the adatom concentration is rather high with the present parameters. We therefore change the parameters to $\phi/k_BT = 3.0$ and τ=4096, which corresponds to x_s=64. With the long diffusion length x_s, grooves may be separated widely from each other. The equilibrium concentration and the equilibrium impingement rate are as small as $c_{\rm eq}$=0.0474 and $f_{\rm eq} = 1.16 \times 10^{-5}$, respectively. The stability limits are $f_{c,[10]} = 1.26 \times 10^{-5}$ in the [10] direction, and $f_{c,[11]} = 1.20 \times 10^{-5}$ in the [11] direction. We hope that the reduction of the impingement rate leads to weakening of the shot noise, and the effect of anisotropy may be easily identified. Figure 5 shows morphologies of [10] and [11] steps in their unstable regions. Figures 5(a) and 5(c) show extended views of size $1024 \times 1024\sqrt{2}$ and 1024×1024 of the [10] step simulated in a system of size $L \times H = 512 \times 512$. Figures 5(b) and 5(d) show extended views of size $512\sqrt{2} \times 1024$ and $512\sqrt{2} \times 512\sqrt{2}$ of the [11] step simulated in a system of size $(L/\sqrt{2}) \times (\sqrt{2}H) = 256\sqrt{2} \times 512\sqrt{2}$. The bars at the upper right of the figures indicate the wavelength of the most unstable mode,

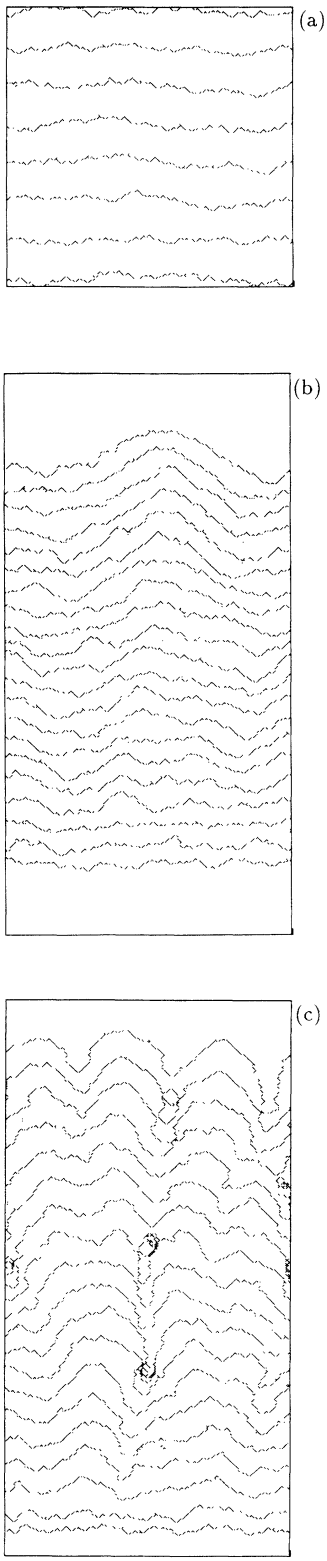

FIG. 4. Time evolution of a single [11] step on a square lattice with parameters $\epsilon/k_BT = \phi/k_BT = 2$, $D_s = 1$, and $\tau = 256$ ($x_s = 16$). Impingement rate is (a) $f = 3 \times 10^{-4}$, (b) $f = 6 \times 10^{-4}$, and (c) $f = 8 \times 10^{-4}$. The step in (a) is receding downward whereas steps in (b) and (c) are advancing upward. The width shown is $256/\sqrt{2}$ in units of the lattice constant, and the heights are $256/\sqrt{2}$ for (a) and $512/\sqrt{2}$ for (b) and (c).

λ_{max}. The final step configuration of each simulation corresponds to (a) $t = 9.30 \times 10^5$, (b) $t = 7.31 \times 10^5$, (c) $t = 5.43 \times 10^4$, and (d) $t = 4.93 \times 10^4$. To generate one data set, diffusion trials up to 10^{11} times are necessary. Near the stability limit $f = 2.5 \times 10^{-5}$ [Figs. 5(a) and 5(b)], both [10] and [11] steps initially develop fluctuations near the most unstable mode ($\lambda_{max} \approx 140$ for [10] and $\lambda_{max} \approx 91$ for [11]). For both steps, growing tips compete with each other and some of them are eliminated at the initial stage. For a [10] step, grooves are constantly produced on the flat top, and thus the separation between neighboring grooves is determined by the diffusional instability to be about λ_{max}. On the other hand, the [11] step in Fig. 5(b) develops into a needlelike form, which seems rather stable. These needles are competing with each other for the available concentration of adatoms, and coarsening takes place as the larger ones grow and widen at the expense of the smaller ones. This coarsening leads to the observed elongation of the needle period for a [11] step.

When the impingement rate is far from the stability limit, such as $f = 8 \times 10^{-5}$, the growth rate is very large and the shot noise associated with the atomic diffusion process is partially frozen in by solidification. Even in this case, the characteristic period of the initial instability seems roughly the same as that of the most unstable mode ($\lambda_{max} \approx 60$ for [10] and $\lambda_{max} \approx 40$ for [11]). When the instability develops, however, the characteristic length of the instability in Fig. 5(c) becomes smaller than λ_{max}. Tips split perpetually for both orientations as is shown in Figs. 5(c) and 5(d). In the early stage of step growth in the [11] direction, dendrites with sidebranches are formed [Fig. 5(d)], but the tip ultimately splits to form an irregular dendrite. The structure looks similar to the random crystal shapes observed in fast crystal growth from a conserved field.[31] Even with random branching of the dendrite, the effect of the crystal anisotropy is still visible. The dendrite branches tend to grow in $\langle 10 \rangle$ directions, while the overall shape is pointed in $\langle 11 \rangle$ directions. This is because the growth in $\langle 10 \rangle$ directions is slower than that in $\langle 11 \rangle$ directions so that the $\{10\}$ faces tend to appear in the crystal form.

In the limit of low temperature, an atom once solidified never melts again. If diffusion is still possible, the diffusional shot noise is frozen as a random shape of the step by the solidification. The formation of a random aggregate by this irreversible solidification and its relation to fractal aggregation[32] are discussed in Ref. 13.

VII. MULTIPLE STEPS

A. Width of a step

We now consider a vicinal surface with an inclination θ from a facet. There are, on the average, $n = d/(a \tan\theta)$ steps on a unit horizontal area with a being the lattice constant in the terrace plane and d the height of the step in the z direction. Average separation between the steps is thus $l = na$. Hereafter we again use a length unit with $a = d = 1$. Because of the overlapping of the diffusion field of neighboring steps, the growth velocity of straight

steps decreases from that of a single step, Eq. (6), by a factor $\tanh(l/x_s)$, and is given by

$$v_0 = \Omega \frac{D_s}{x_s}(c_\infty - c_{\rm eq}) \tanh \frac{l}{x_s}, \tag{42}$$

where the kinetic coefficients are set $K_- = 0$ and $K_+ = \infty$, corresponding to the one-sided model. This reduction of the step advancement velocity for $f > f_{\rm eq}$ is evident from the Monte Carlo data shown in Fig. 6(a). On decreasing the step separation l, one also notices the better agreement of the simulated velocity with the theoretical one. This is due to the smoothing of the step as described below.

We have analyzed[11,12] the stability of sequences of straight steps with equal separation l. Assuming *in-phase*

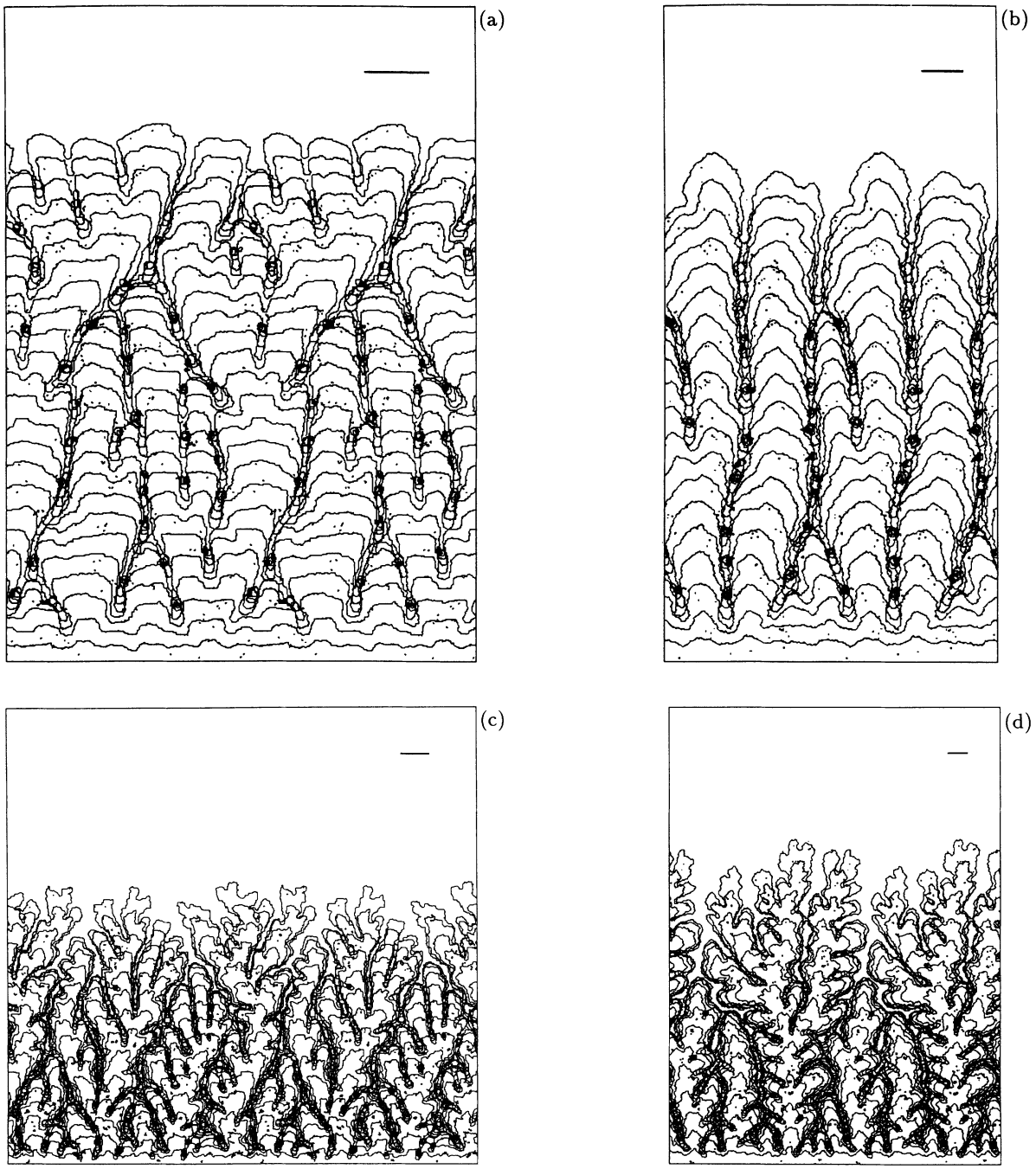

FIG. 5. Time evolution of a single step on a square lattice with parameters $\epsilon/k_BT = 2$, $\phi/k_BT = 3$, $D_s = 1$, and $\tau = 4096$ ($x_s = 64$). Step orientation is [10] for (a) and (c) with width 1024, and [11] for (b) and (d) with width $512\sqrt{2}$. Impingement rate is $f = 2.5 \times 10^{-5}$ (a,b) and $f = 8 \times 10^{-5}$ (c,d). The bars indicate the wavelength of the fastest growing mode $\lambda_{\rm max}$.

deformation the mth step deforms as

$$y_m(x,t) = ml + v_0 t + \delta y_k e^{\omega_k t} \cos kx. \tag{43}$$

The amplification factor ω_k is factorized into the mobility $\mu_k(l)$ and the effective force constant $\nu_k^{(+)}(f;l)$ for the in-phase mode, as $\omega_k = -\mu_k(l)\nu_k^{(+)}(f;l)$ with[9]

$$\mu_k(l) = \Omega^2 \frac{c_{\rm eq}^0}{k_B T} D_s \Lambda_k \tanh(\Lambda_k l) \tag{44}$$

and

$$\nu_k^{(+)}(f;l) = \tilde{\beta}\left[k^2 - \frac{x_s\Lambda_k \tanh(l/x_s)\tanh(\Lambda_k l) - 1 + \mathrm{sech}(l/x_s)\mathrm{sech}(\Lambda_k l)}{\xi x_s^2 \Lambda_k \tanh(\Lambda_k l)}\right]. \tag{45}$$

For small k, $\nu_k^{(+)}(f;l)$ can be expanded as before as $\nu_k^{(+)}(f;l) = \tilde{\beta}_{\rm eff}(f;l)k^2 + O(k^4)$ with the effective step stiffness now modified as

$$\tilde{\beta}_{\rm eff}(f;l) = \tilde{\beta}\left(1 - \frac{x_s}{2\xi(f)} \tanh\frac{l}{x_s}\right). \tag{46}$$

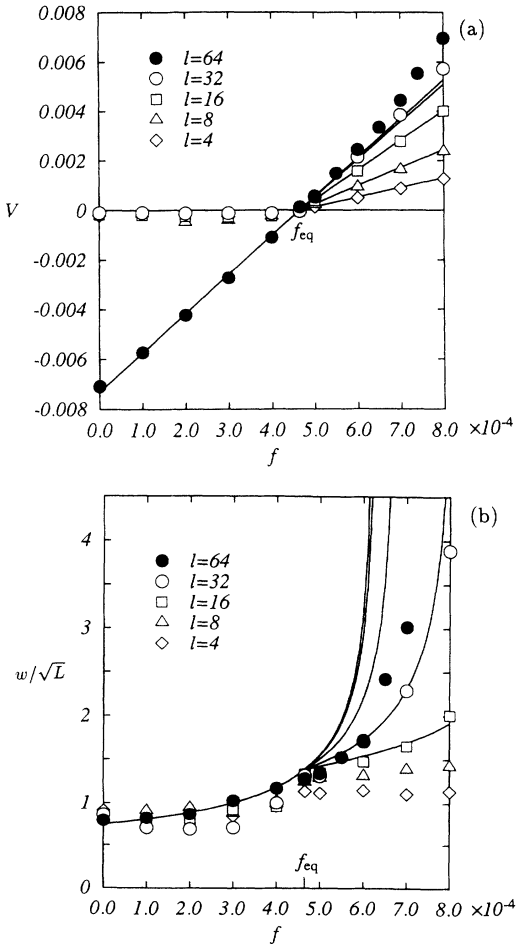

FIG. 6. (a) Growth velocity and (b) the width of a step in a multiple [10] step system versus the impingement rate f. The system size is $L \times H = 64 \times 64$. Parameters are $\epsilon/k_BT = \phi/k_BT = 2$, $D_s = 1$, and $\tau = 256$ ($x_s = 16$), and the average step distances are $l = 64$ (•), 32 (○), 16 (□), 8 (△), and 4 (◇). The simulation data show qualitatively the same tendency as the theoretical curves.

The instability then takes place at $\tilde{\beta}_{\rm eff}$=0 or

$$f_c = f_{\rm eq}\left[1 + \frac{2\Omega\tilde{\beta}}{k_B T x_s \tanh(l/x_s)}\right]$$

$$\to f_{\rm eq}\left(1 + \frac{2\Omega\tilde{\beta}}{k_B T x_s}\right) \quad \text{for } l \gg x_s, \tag{47}$$

$$\to f_{\rm eq}\left(1 + \frac{2\Omega\tilde{\beta}}{k_B T l}\right) \quad \text{for } l \ll x_s. \tag{48}$$

When the separation between steps, l, is large compared with the diffusion length x_s, each step is apparently independent and the critical point f_c is the same as that for a single step. When the separation l is smaller than x_s, on the other hand, the diffusion field of neighboring steps overlaps to suppress the instability, and the critical impingement rate f_c increases compared with that of an isolated step. This effect has been studied by Bales and Zangwill.[9]

Associated with the above instability we expect an enhancement of the step width as before. Assuming that a small deviation δy_k from the straight step follows the same evolution equation (32) but with the modification of μ_k and ν_k given in Eqs. (44) and (45), the width of each step takes the form $w^2 = L^{-1}\sum_k \langle|\delta y_k|^2\rangle \approx Lk_BT/12\tilde{\beta}_{\rm eff}(f;l)$, with the effective step stiffness given by Eq. (46). For a fixed f between $f_{\rm eq}$ and f_c, the step width $w/\sqrt{L}$ of multiple steps is suppressed compared with that for an isolated step. Monte Carlo simulation for SOS steps[11,12] has shown this tendency of width suppression on increasing the step density for $f > f_{\rm eq}$, as is shown in Fig. 6. However, for $f < f_{\rm eq}$ we encounter another step instability which leads to bunching of steps. We describe it later, in Sec. VII C.

Even for $f > f_{\rm eq}$ the width analysis with Eq. (35) is not correct for a large system. In Eq. (35) the interaction of steps via the diffusion field is included, but direct interaction of steps via a hard core or the prohibition of step overlapping is neglected. Steps separated by a distance l can fluctuate freely up to a step length of order l^2, but for a longer scale collision of steps suppresses the fluctuation. Since the height fluctuation of a vicinal rough surface for a system with size L is known to be propor-

tional to $\ln L$, the step fluctuation may well be limited by $\ln L$ asymptotically for $L \gg l^2$, at least in equilibrium.[33]

B. Fluctuation of step separation

A novel aspect of a multiple step system is the correlation among steps. One may intuitively expect that the correlation of neighboring steps becomes strong when the separation between the steps l becomes small, or when the impingement rate f increases. This correlation is reflected in the fluctuation of the separation of consecutive steps: $\hat{l}(x,t) = y_m(x,t) - y_{m-1}(x,t)$. In Fig. 7, where snapshots of a multiple step system are shown, the fluctuation of each step looks larger for $f = 6.0 \times 10^{-4}$ [Fig. 7(c)] than that for $f = 4.65 \times 10^{-4}$ [Fig. 7(b)], but the fluctuation of the separation of steps (or the terrace width) looks smaller for $f = 6.0 \times 10^{-4}$. This visual impression is confirmed by taking statistics of the distribution of the step separation as shown in Figs. 8(a) and 8(c). At the equilibrium impingement rate $f = 4.65 \times 10^{-4}$, the distribution is asymmetric and agrees with that of the free-fermion model calculated by Joós, Einstein, and Bartelt.[8] This is natural because equilibrium fluctuation is independent of dynamics as long as the energy associated with the fluctuation does not depend on the dynamics. On increasing the impingement rate the distribution becomes similar to the Gaussian and the standard deviation decreases drastically. Although the width of individual steps increases in growth, the terrace width becomes homogeneous with small fluctuation. In order to understand this nonequilibrium phenomenon we develop a mean-field theory.

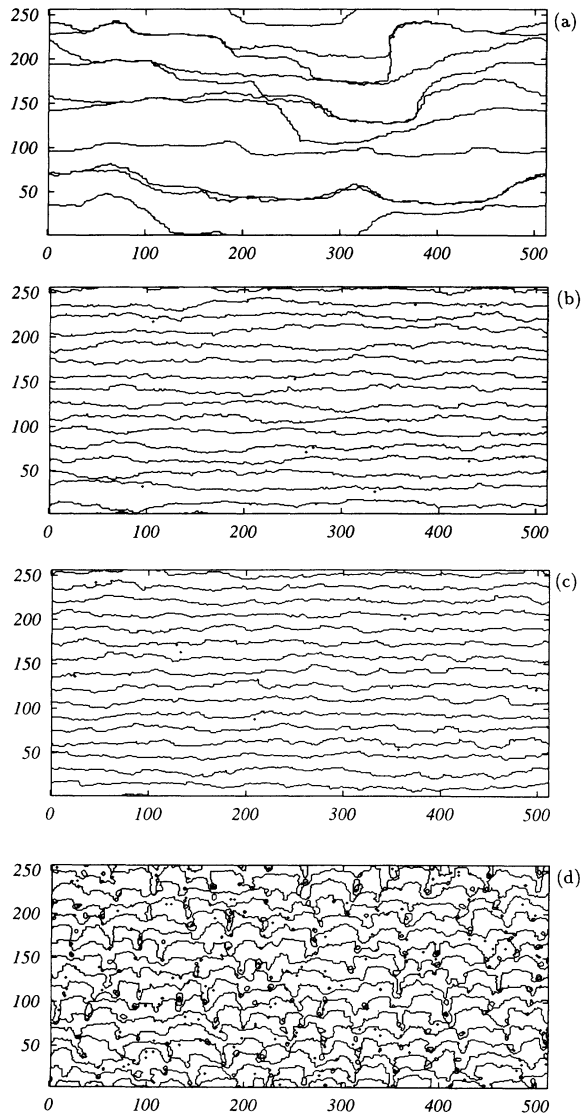

FIG. 7. Snapshot configuration of 16 [10] steps on a square lattice with parameters $\epsilon/k_BT = \phi/k_BT = 2$, $D_s = 1$, and $\tau = 256$ ($x_s = 16$) for a system size $L \times H = 512 \times 256$. Impingement rates are (a) $f = 0$, (b) $f = f_{eq} = 4.65 \times 10^{-4}$, (c) $f = 6 \times 10^{-4}$, and (d) $f = 10 \times 10^{-4}$. In (a) only 10 steps can be identified because of the multiple bunching.

The effect of neighboring steps on the fluctuation of a central step is twofold: the equilibrium interaction and the interference of the diffusion field in growth. In the mean-field picture, we consider a step on a vicinal surface as one fluctuating under the influence of other steps which are fixed at their average position. The condition that the steps cannot cross gives rise to a statistical interaction.[34] For an array of steps this leads to an increase in the free energy per unit area by[5,6] $(\pi^2/6)(k_BT)^2/\tilde{\beta}l^3$. We will find an effective one-body potential which produces the equivalent free-energy increase. If a two-body potential between steps separated by a distance l has the form $U(l) = Al^{-n}$, the displacement of a central step, $\delta y(x)$, yields the effective one-body potential

$$V(\delta y) = \sum_{m=1}^{\infty} [U(ml + \delta y) + U(ml - \delta y)]$$
$$= 2\zeta(n)\frac{A}{l^n} + n(n+1)\zeta(n+2)\frac{A}{l^{n+2}}(\delta y)^2, \quad (49)$$

where $\zeta(n)$ is the Riemann zeta function. The first term gives the interaction per step with the separation l. Comparing this term with the increase in the free energy we conclude that the statistical interaction corresponds to an effective potential with $n = 2$ and $A = (k_BT)^2/\tilde{\beta}$. Near the equilibrium position $\delta y(x) = 0$, the harmonic potential $V(\delta y) \approx (1/2)V''(0)\delta y^2$ yields a restoring force $-V'(\delta y) = -V''(0)\delta y(x)$, which changes the local equilibrium density as[17]

$$c_{eq} = c_{eq}^0 + \frac{\Omega c_{eq}^0}{k_BT}[\tilde{\beta}\kappa + V''(0)\delta y(x)]. \quad (50)$$

As for the dynamical effect of the diffusion field, we calculate the growth rate of the step fluctuation similarly as in Sec. VII A, but *with fixed neighbors*. The mobility is the same as Eq. (43) and the restoring force is

$$\nu_k^{(0)}(f;l) = \tilde{\beta}\left[k^2 - \frac{x_s\Lambda_k \tanh(l/x_s)\tanh(\Lambda_k l) - 1}{\xi x_s^2 \Lambda_k \tanh(\Lambda_k l)} + \frac{2\pi^4}{15}\frac{k_B^2T^2}{\tilde{\beta}l^4}\right]. \quad (51)$$

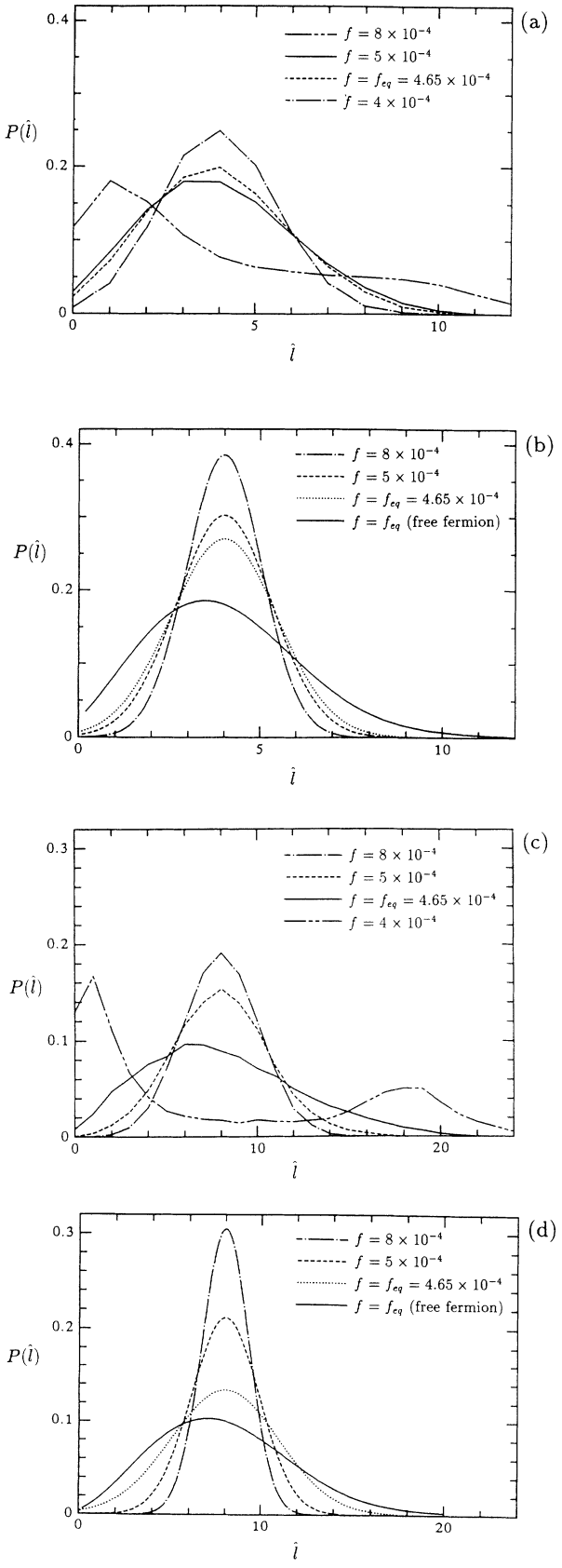

FIG. 8. Comparison of terrace width distribution $P(\hat{l})$ obtained by simulation (a), (c), and by the theory (b), (d), in a multiple step system with average step separations $l = 4$ (a,b) and $l = 8$ (c,d).

The third term in the bracket is due the the mean-field statistical repulsion. The diffusion field provides an additional force, the second term. It is attractive when $\xi < 0$ and is repulsive when $\xi > 0$. We can calculate the standard deviation σ of the terrace distribution using the same formula (35) with Eq. (51), replacing w by σ. The result is shown in Figs. 8(b) and 8(d). Compared with the simulation result, Figs. 8(a) and 8(c), the mean-field approximation with fixed neighbors obviously produces a sharper peak in the terrace width distribution due to overestimation of the correlation, but the qualitative tendency of the fluctuation suppression for large f is well reproduced.

One can understand the result easily. If $l \ll x_s$ the statistical repulsion and the interference of the diffusion field produce the effective dynamical potential in the limit of $k \to 0$ as

$$V_d''(0) = \nu_0^{(0)}(f;l) = \frac{2\pi^4 k_B^2 T^2}{15 l^4} + \frac{\tilde{\beta}}{\xi l}. \tag{52}$$

Then the Hamiltonian for small-amplitude fluctuation δy_k is

$$H = \sum_k [\tfrac{1}{2}\tilde{\beta}k^2 + \tfrac{1}{2}V_d''(0)]|\delta y_k|^2. \tag{53}$$

Thus the distribution of $\delta y(x)$ is Gaussian,[7] and the standard deviation σ is calculated as

$$\begin{aligned}\sigma^2 &\equiv \langle [y_m(x) - y_{m-1}(x)]^2 \rangle \\ &= 2\int_{-\pi/L}^{\pi/a} \frac{k_B T}{\tilde{\beta}k^2 + V_d''(0)} \frac{dk}{2\pi} \approx \frac{k_B T}{2\sqrt{\tilde{\beta} V_d''(0)}},\end{aligned} \tag{54}$$

where the range of integration has been extended from 0 to ∞. In equilibrium, Eq. (54) becomes $\sigma = (15/8)^{1/4}\pi^{-1} l = 0.372l$, which is independent of $\tilde{\beta}$ and T and proportional to l, in qualitative agreement with the rigorous behavior. Only the coefficient is a little smaller than the exact value for the free-fermion model,[8] 0.424. When the step is advancing, the diffusion field produces additional repulsion in growth ($\xi > 0$), and σ becomes smaller as the impingement rate f is increased (i.e., ξ is decreased).

C. Step bunching

The repulsive interaction which stabilizes the step separation turns into an attractive interaction when steps are sublimating for f smaller than f_{eq} with a negative ξ. This attractive interaction causes bunching of steps. The relevant mode of fluctuation now is the *antiphase* oscillation of consecutive steps:

$$y_m(x,t) = ml + v_0 t + (-1)^m \delta y_k e^{\omega_k t} \cos kx. \tag{55}$$

From the linear analysis we obtain the dispersion $\omega_k = -\mu_k(l)\nu_k^{(-)}(f;l)$ with the new restoring force

$$\nu_k^{(-)}(f;l)=\tilde{\beta}\left[k^2-\frac{x_s\Lambda_k\tanh(l/x_s)\tanh(\Lambda_k l)-1-\mathrm{sech}(l/x_s)\mathrm{sech}(\Lambda_k l)}{\xi x_s^2\Lambda_k\tanh(\Lambda_k l)}\right]\approx\tilde{\beta}\left(k^2+\frac{2}{\xi l}\right). \tag{56}$$

If we do not include the statistical repulsion, which would appear as $\pi^4 k_B^2 T^2/8\tilde{\beta}l^4$ for this mode, the long-wavelength fluctuation is always unstable as soon as $f<f_{\rm eq}$ or $\xi<0$. The most dangerous mode with the largest ω_k is the uniform mode with $k=0$, and thus neighboring steps approach and separate from each other alternately. This represents the instability of neighboring steps against pairing.[16] Even with repulsive step interaction, the same step pairing occurs if the impingement rate is smaller than a critical value.[18]

In the simulation, we observe bunched steps which move very slowly. If there were no thermal fluctuation, steps would stop moving with our simulation algorithm. These paired steps make a peak at zero separation in the distribution of the step separation for $f<f_{\rm eq}$ in Fig. 8. If a single step remains unpaired, it recedes fast, and overtakes and collides with a slow pair to emit a freed step from the opposite end, just like a billiard ball collision.[17] If the system width L is narrow, the bunching takes place for the whole width of the system,[12] but for a wide system the bunching will happen here and there inhomogeneously and a connected network of steps is formed, as is shown in Fig. 7(a).

VIII. SUMMARY

Steps growing in a diffusion field show a diversity of morphologies and dynamics. We have shown that the fluctuation is reduced when the step is sublimating, whereas it is enhanced when the step is advancing in growth. This effect is observable by direct methods such as the STM, AFM, or electron microscopes. The change in the surface roughness also affects the scattering intensity such as that in reflection high-energy electron diffraction or ion-beam scattering experiments. Calculation of the scattering intensity $I(\mathbf{q})$ with a momentum transfer $\mathbf{q}$ is briefly summarized in the Appendix. For step sequences with separation l in the y direction, scattering consists of peaks at $q_x=0$, $lq_y+q_zd=2\pi m$ with integer values of m. The decay of the peak intensity in the q_y direction is characterized by fluctuation of the terrace width σ, whereas the width in the q_x direction is characterized by the fluctuation of a single step w. Therefore, reflecting the value of w, the peak becomes sharp for a sublimating step, and becomes diffuse for growing steps. The change will be drastic near the morphological instability at f_c. Since the radius of the critical two-dimensional nucleus ξ is a half of the surface diffusion length x_s even at the critical point, this kinetic roughening should not be hidden by two-dimensional nucleation on terraces as long as the Schwoebel effect dominates. The detailed features of the scattering peaks, however, require more study since the assumption (A4) in the Appendix is correct only at short distances, as explained at the end of Sec. VII A. For equilibrium steps, the scattering intensity has been calculated with a correct asymptotic formula.[35]

In addition to the steady-state behavior, one can also study relaxation or transient behavior with our time-dependent correlation function of Eq. (33). Recently Salditt and Spohn[36] studied the initial increase of roughness (step width) w with a similar equation analytically and by a Monte Carlo simulation, and found three different regimes: $w\sim t^{1/6}$ for diffusion control, $w\sim t^{1/4}$ for kinetics control, and $w\sim t^{1/3}$ for a nonlinearity control regime. Their result for the steady-state step width is, however, different from ours. The origin of their noise is nonthermal in the impingement rate f and they neglected thermal fluctuations due to melting and crystallization at the step. As a result the step fluctuation is simply proportional to f, vanishes at $f=0$, and does not show any critical behavior at f_c. Therefore we believe that our Langevin-type theory satisfying the fluctuation-dissipation relation is more realistic in this respect.

According to our linear analysis, the effective stiffness of an isolated step, $\tilde{\beta}_{\rm eff}$, Eq. (16), decreases near the critical point and the width diverges at the critical impingement rate f_c in a power law $w^2\propto(f_c-f)^{-1}$. Near the criticality, however, nonlinearity of the step fluctuation should be important, and a reductive perturbation calculation leads to evolution of the step fluctuation $Y(x,t)=y(x,t)-v_0t$ as

$$\frac{1}{\mu_0}\frac{\partial Y}{\partial t}=2\tilde{\beta}_{\rm eff}\frac{\partial^2 Y}{\partial x^2}-\frac{3}{4}\tilde{\beta}x_s^2\frac{\partial^4 Y}{\partial x^4}+\frac{\tilde{\beta}}{x_s}\left(\frac{\partial Y}{\partial x}\right)^2+R(x,t), \tag{57}$$

with the thermal fluctuation $R(x,t)$. For $f<f_c$ with positive $\tilde{\beta}_{\rm eff}$, the interface is stable and the fourth derivative may be negligible, and Eq. (57) reduces to the Kardar-Parisi-Zhang (KPZ) equation.[37] The interface fluctuation w^2 is proportional to the system width L, consistent with the KPZ result. Above the instability, $f>f_c$, however, the fourth derivative is inevitable and the system is governed by the Kuramoto-Sivashinski equation. The scaling behavior of w^2 of the noise-affected KS equation is an interesting future problem.

The dynamics and the morphology of a step are also influenced by anisotropy. The crystalline anisotropy reveals itself in a difference of step stiffness, and thus in the fluctuation or width of a stable step as well as in the modification of the step velocity. When step instability takes place, the anisotropy effect seems prominent. The [10] step with a flat top shows spatiotemporal chaotic behavior near f_c, whereas the [11] step with a pointed top shows more regular behavior, indicating the tip stabilization effect of the stiffness anisotropy. However, due to the strong and uncontrollable shot noise caused by solidification as well as the incommensurability of the system size to the period of the stable structure, the [11] step

also sometimes shows tip-splitting instability. For large f the step forms a dendrite with rather random branching. The morphological features seen in the simulation may be observed in thin-film growth. Transmission electron microscope pictures[38] of tungsten crystals of $A15$ structure grown on KCl show a morphology in common with our simulation.

For a vicinal face or a multiple step system with a step separation l smaller than the diffusion length x_s, the overlapping of the diffusion field influences the stability and the morphology of steps. For an advancing step, the individual step fluctuation or the width is suppressed by the competition among neighboring steps. By increasing the impinging flux f, the step fluctuation increases but the fluctuation of the terrace width decreases. This is due to kinetically enhanced coherence among steps, which leads to reduction of out-of-phase fluctuations between neighboring steps during advancement. The antiphase fluctuation, on the other hand, leads to bunching instability for receding or sublimating steps. Bunching of sublimating steps is often observed on Si surfaces. For a quantitative explanation of real phenomena, one may need the repulsive interaction among steps as well as the exchange of atoms with the upper terrace. Also, our analysis of the step correlation is based on mean-field analysis and Monte Carlo simulation. The former is essentially a one-step picture and the latter is limited by size, and thus additional considerations are required for the *asymptotic* behavior.[39]

ACKNOWLEDGMENTS

The authors thank A. Ichimiya for discussions on RHEED and S. Nishikawa for video recording of the simulation result. Y.S. acknowledges a fruitful discussion with C. Misbah. The work is supported by Grants-in-Aid for Scientific Research on Priority Areas from the Ministry of Education, Science and Culture of Japan (No. 03243101 and No. 04227108). A part of the work was done under the interuniversity cooperative research program of the Institute for Materials Research of Tohoku University. M.U. thanks the Foundation for Promotion of Material Science and Technology of Japan for financial support.

APPENDIX

We summarize briefly the calculation of the scattering intensity in the eikonal approximation. The formula may be applicable to reflection high-energy electron diffraction or low-energy atomic-beam diffraction. By denoting the momentum transfer $\mathbf{q} = (q_x, q_y, q_z)$, the scattering function is written as[40,41]

$$I(\mathbf{q}) = \frac{1}{LH}\sum_{\mathbf{r}}\sum_{\mathbf{r}'}\langle \exp[iq_x(x-x') + iq_y(y-y') + iq_z(z(x,y)-z(x',y'))]\rangle$$
$$= \frac{1}{LH}\left\langle \left| \int dx \int dy \exp[iq_x x + iq_y y + iq_z z(x,y)] \right|^2 \right\rangle. \tag{A1}$$

Since the crystal height is $z(x,y) = z_0 + m$ for the mth terrace, with $y_m(x) < y < y_{m+1}(x)$, the integral becomes

$$\int dx \int dy \exp[iq_x x + iq_y y + iq_z z(x,y)] = e^{iq_z z_0} \int dx \sum_m \int_{y_m(x)}^{y_{m+1}(x)} dy e^{iq_x x + iq_y y + iq_z m}$$
$$= \frac{e^{iq_z z_0}}{iq_y} \int dx e^{iq_x x} \sum_m e^{iq_z m}(e^{iq_y y_{m+1}(x)} - e^{iq_y y_m(x)}), \tag{A2}$$

and the scattering intensity is calculated as[42]

$$I(\mathbf{q}) = \frac{2(1-\cos q_z)}{lq_y^2} \int dx e^{iq_x x} \sum_{m=0}^{H/l-1} e^{iq_z m} e^{iq_y ml} \langle e^{iq_y(\delta y_m(x) - \delta y_0(0))}\rangle. \tag{A3}$$

Here the location of the mth step is written as $y_m(x) = ml + \delta y_m(x)$ with the average step separation l. The thermal average is calculated by using the cumulant expansion, as

$$\langle e^{iq_y(\delta y_m(x) - \delta y_0(0))}\rangle \approx \exp\left[-\frac{q_y^2}{2}\langle[\delta y_m(x) - \delta y_0(0)]^2\rangle\right]$$
$$= \exp\left[-\frac{q_y^2}{2}\langle[\delta y_m(x) - \delta y_0(x) + \delta y_0(x) - \delta y_0(0)]^2\rangle\right]$$
$$\approx \exp\left(-\frac{q_y^2}{2}\{\langle[\delta y_m(x) - \delta y_0(x)]^2\rangle + \langle[\delta y_0(x) - \delta y_0(0)]^2\rangle\}\right),$$

where we have neglected the correlation between the terrace width fluctuation and that of a single step: $\langle[\delta y_m(x) - \delta y_0(x)][\delta y_0(x) - \delta y_0(0)]\rangle$. If we assume that the fluctuation of the step separation is independent and is given by σ^2 and that the correlation within a step (38) is approximated by its effective stiffness, we obtain

$$\langle e^{iq_y(\delta y_m(x)-\delta y_0(0))}\rangle \approx \exp\left[-\frac{q_y^2}{2}\sigma^2|m| - \frac{q_y^2}{2}\frac{k_BT}{\tilde{\beta}_{\rm eff}}|x|\right]. \tag{A4}$$

Thus the scattering function is calculated for a large system ($H \to \infty$) as

$$I(\mathbf{q}) = \frac{2k_BT(1-\cos q_z d)}{\tilde{\beta}_{\rm eff} l} \times \frac{1-e^{-q_y^2\sigma^2}}{1-2e^{-q_y^2\sigma^2/2}\cos(q_z d + q_y l) + e^{-q_y^2\sigma^2}} \times \frac{1}{q_x^2 a^2 + (q_y^2 k_BT/2\tilde{\beta}_{\rm eff})^2}, \tag{A5}$$

where the lattice constants a and d are inserted. In the limit of vanishing q_y, with the use of the formula

$$\frac{2q_y}{X^2+q_y^2} \to 2\pi\delta(X),$$

the scattering intensity is calculated as

$$I(q_x,0,q_z) = (2\pi)^2 l\delta(q_x a)\sum_n \delta(q_z d - 2\pi n) + 2\pi\frac{\sigma^2}{l}\delta(q_x a). \tag{A6}$$

The approximations we made here are not very good, as discussed at the end of Sec. VII A but effective for a qualitative analysis. For a given q_z the scattering function consists of peaks at $q_y = (2\pi m - q_z d)/l$ with integer values of m, representing the periodic arrangement of steps with periodicity l in the y direction. The peak intensity decays very rapidly as m increases unless q_y is very small. The width in the q_x direction is $q_y^2 k_BT/2\tilde{\beta}_{\rm eff} = 6q_y^2 w^2/L$, which diverges on approaching the instability of the straight step at $f = f_c(l)$. On the other hand, for a sublimating step, $\tilde{\beta}_{\rm eff}$ increases and the peak sharpens.

* Present address: Department of Physics, Nagoya University, Furo-cho, Chikusa-ku, Nagoya 464-01, Japan.

[1] A. V. Latyshev, A. L. Aseev, A. B. Krasilnikov, and S. I. Stenin, Surf. Sci. **213**, 157 (1989).
[2] B. S. Schwartzentruber, Y.-W. Mo, R. Kariotis, M. G. Lagally, and M. B. Webb, Phys. Rev. Lett. **65**, 1913 (1990).
[3] X. S. Wang, J. L. Goldberg, N. C. Bartelt, T. L. Einstein, and E. D. Williams, Phys. Rev. Lett. **65**, 2430 (1990).
[4] C. Alfonso, J. M. Bermond, J. C. Heyraud, and J. J. Métois, Surf. Sci. **262**, 371 (1992).
[5] T. Yamamoto, Y. Akutsu, and A. Akutsu, J. Phys. Soc. Jpn. **57**, 453 (1988).
[6] Y. Akutsu, A. Akutsu, and T. Yamamoto, Phys. Rev. Lett. **61**, 424 (1988).
[7] N. C. Bartelt, T. L. Einstein, and E. D. Williams, Surf. Sci. Lett. **240**, L591 (1990).
[8] B. Joós, T. L. Einstein, and N. C. Bartelt, Phys. Rev. B **43**, 8153 (1991).
[9] G. S. Bales and A. Zangwill, Phys. Rev. B **41**, 5500 (1990). [There are a few misprints in Eqs. (18) and (20) of this paper. See Phys. Rev. B **48**, 2024(E) (1993).]
[10] M. Uwaha and Y. Saito, Phys. Rev. Lett. **68**, 224 (1992).
[11] M. Uwaha and Y. Saito, Surf. Sci. **283**, 366 (1993).
[12] M. Uwaha and Y. Saito, J. Cryst. Growth **128**, 87 (1993).
[13] Y. Saito, T. Sakiyama, and M. Uwaha, J. Cryst. Growth **128**, 82 (1993).
[14] R. Trivedi, Metall. Trans. A **15**, 977 (1984).
[15] Y. Saito, C. Misbah, and H. Müller-Krumbhaar, Phys. Rev. Lett. **63**, 2377 (1989).
[16] P. Bennema and G. H. Gilmer, in *Crystal Growth: An Introduction*, edited by P. Hartman (North-Holland, Amsterdam, 1973), p. 263.
[17] M. Uwaha, Phys. Rev. B **46**, 4364 (1992).
[18] M. Uwaha, J. Cryst. Growth **128**, 92 (1993).
[19] W. K. Burton, N. Cabrera, and F. C. Frank, Philos. Trans. R. Soc. London, Ser. A **243**, 299 (1951).
[20] R. L. Schwoebel and E. J. Shipsey, J. Appl. Phys. **37**, 3682 (1969).
[21] J. Villain, J. Phys. I (France) **1**, 19 (1991).
[22] P. Nozières and F. Gallet, J. Phys. (Paris) **48**, 353 (1987).
[23] H. J. Leamy, G. H. Gilmer, and K. A. Jackson, in *Surface Physics of Materials*, edited by J. M. Blakely (Academic, New York, 1975), Vol. 1, pp. 121–188.
[24] J. M. Flesselles, A. J. Simon, and A. J. Libchaber, Adv. Phys. **40**, 1 (1991).
[25] I. Bena, C. Misbah, and A. Valance, Phys. Rev. B **47**, 7408 (1993).
[26] Y. Kuramoto and T. Tsuzuki, Prog. Theor. Phys. **55**, 356 (1976).
[27] G. I. Sivashinsky, Acta Astronaut. **4**, 1177 (1977).
[28] P. Manneville, *Dissipative Structures and Weak Turbulence* (Academic, San Diego, 1990).
[29] J. S. Langer, in *Le Hazard et la Matière*, edited by J. Souletie, J. Vannimenus, and R. Stora (North-Holland, Amsterdam, 1987), p. 629.
[30] This formula [Eq. (36) as well] is for SOS step. The step stiffness for a non-SOS step is calculated in Y. Akutsu and N. Akutsu, J. Phys. A **19**, 2813 (1986), and yields $k_BT/\tilde{\beta}_{[10]} = 0.367$ and $k_BT/\tilde{\beta}_{[11]} = 0.823$.
[31] Y. Saito and T. Ueta, Phys. Rev. A **40**, 3408 (1989).
[32] M. Uwaha and Y. Saito, J. Phys. Soc. Jpn. **51**, 3285 (1988); Phys. Rev. A **40**, 4716 (1989).
[33] This has been demonstrated for the free-fermion model and for the capillary model: N. C. Bartelt, T. L. Einstein, and E. D. Williams, Surf. Sci. **276**, 308 (1992); T. Yamamoto, Y. Akutsu, and N. Akutsu, J. Phys. Soc. Jpn. (to be pub-

lished).
[34] E. E. Gruber and W. W. Mullins, J. Phys. Chem. Solids **28**, 875 (1967).
[35] N. C. Bartelt, T. L. Einstein, and E. D. Williams, Surf. Sci. **244**, 149 (1991).
[36] T. Salditt and H. Spohn, Phys. Rev. E **47**, 3524 (1993).
[37] M. Kardar, G. Parisi, and Y. C. Zhang, Phys. Rev. Lett. **56**, 889 (1986).
[38] M. Arita and I. Nishida (unpublished).
[39] D. E. Wolf, Phys. Rev. Lett. **67**, 1783 (1991).
[40] G. Blatter, Surf. Sci. **145**, 419 (1984).
[41] A. Ichimiya, Surf. Sci. **187**, 194 (1987).
[42] J. Villain, D. R. Grempel, and J. Lapujoulade, J. Phys. F **15**, 809 (1985).